Synergic analytical strategy to follow the technological evolution of Campanian medieval glazed pottery

Lorena Carla Giannossa[1] · Maria Cristina Caggiani[2] · Rocco Laviano[3] ·Pasquale Acquafredda[3] · Marcello Rotili[4] · Annarosa Mangone[1]

[1] Dipartimento di Economia, Management e Diritto dell'Impresa,Università degli Studi di Bari Aldo Moro, Bari, Italy
[2] Dipartimento di Chimica, Università degli Studi di Bari Aldo Moro,Bari, Italy
[3] Dipartimento di Scienze della Terra e Geoambientali, Universitàdegli Studi di Bari Aldo Moro, Bari, Italy
[4] Dipartimento di Lettere e Beni Culturali, Università degli Studi dellaCampania, Caserta, Italy

Abstract Three classes of medieval lead-tin-glazed ceramics(protomajolica, transition enamel pottery and white enamel pottery), from the archaeological site of Castello del Monte in Montella (Avellino, southern Italy), were investigated. Inductively coupled plasma–mass spectrometry (ICP-MS), optical and scanning electron microscopy with energy- dispersive X-ray spectroscopy (OM and SEM-EDS) and X-ray powder diffraction (XRPD) were carried out on ceramicbodies, coatings and decorations in order to outline the technological features and define the nature of glazes and pigments. The aim of this work, in addition to delineating the features of production, is to confirm the archaeological hypothesis that transition enamel pottery produced between thefourteenth and fifteenth centuries, although having much incommon with the protomajolica, is in fact a version of whiteenamel pottery, characterised by morphological and ornamental diversity. Our results show that both ceramic bodies andcoatings feature different structural and compositional characteristics, linking the three ceramic classes and making it possible to confirm the archaeological hypothesis that transition enamel pottery can be defined as a ceramic class with transitional features between protomajolica and white enamel pottery.

Keywords Campanian medieval glazed pottery, X-raydiffraction, Ceramic classes

Introduction

The archaeological excavations in Castello del Monte in Montella (Avellino, South Italy) are part of a number of investigations of medieval settlements carried out for more than 30 years in northern Irpinia (Rotili 1999). The town of

Montella originally grew from the joining of various late medieval farmhouses located in the valley of the Santa Maria stream. Archaeological research has made it possible to reconstructthe most significant phases of the history of the del Monte building which was first occupied in the sixth–seventh centuries as a consequence of the abandonment of the valley floor atthe end of the ancient times. Fortified in the the ninth century and adapted to suit the administrative and military necessities of managing the territory, the hill settlement assumed the characteristics of a microurban structure. In the first half of the twelfth century, it was the location of a castle whose residential tower (*donjon*), with a circular ground plan, was particularly evident. After its assignment to members of the Angevin house in the second half of the thirteenth–fourteenth centuries,the tower was renovated, the rooms were enlarged and the *palatium* was built; the defensive structures were improvedand the whole area was terraced, making it a hunting reserveadorned with aqueducts and fountains. The castle and the delMonte settlement were seriously damaged during the Franco- Imperial conflicts, particularly during Count Lautrec's mission during the first half of the sixteenth century. Followingthis, they were gradually abandoned and the valley floor wasrepopulated.

Archaeological excavation of the site has centred on the *donjon*, the *palatium*, the castle's numerous rooms and its *rasole* (a word that in the eighteenth century indicated the Angevin age terracings), bringing to light huge quantities ofpottery and other findings.

For the purpose of this study, the findings which have beenexamined belong to particularly important ceramic classes produced between the thirteenth and sixteenth centuries. They provide much information concerning life in MontellaCastle during the Middle Ages. The items show an evolutionary trend from the first evidence of glazed pottery with polychrome decorations and the well-known *protomajolica* (dating from the second half of the thirteenth century to the early fourteenth century) to transitional glazed products (four- teenth–sixteenth centuries) and vessels of the Modern Era, such as white enamel or white enamel with blue motives pottery (beginning of sixteenth century AD). Based on comparisons with fine ceramics coming from neighbouring areas, we realised that vessels from Montella are part of a wider production, which was to a great extent evenly distributed in the hinterland of Campania. At the end of the thirteenth century,this macro-area (Fig. 1) included manufacturing centres suchas Ariano Irpino, whose tax records highlight an intense productive and commercial activity (Bevere 1940). The high level of quality and the commercial success achieved by *protomajolica* and transition enamel pottery from Irpinia are documented by the presence of ceramic imitations, which evoke the ornamental motives of *protomajolica* but which are made with less expensive materials.

Whereas vascular and decorative repertoires of these ceramic classes have been the subject of an appropriate and critical

overview, there is an almost total lack of data regardingmanufacturing locations. Therefore, we know of little aboutthe dynamics of production and circulation of tableware in theApennines of Campania and nearby areas between the medi-eval and modern ages.

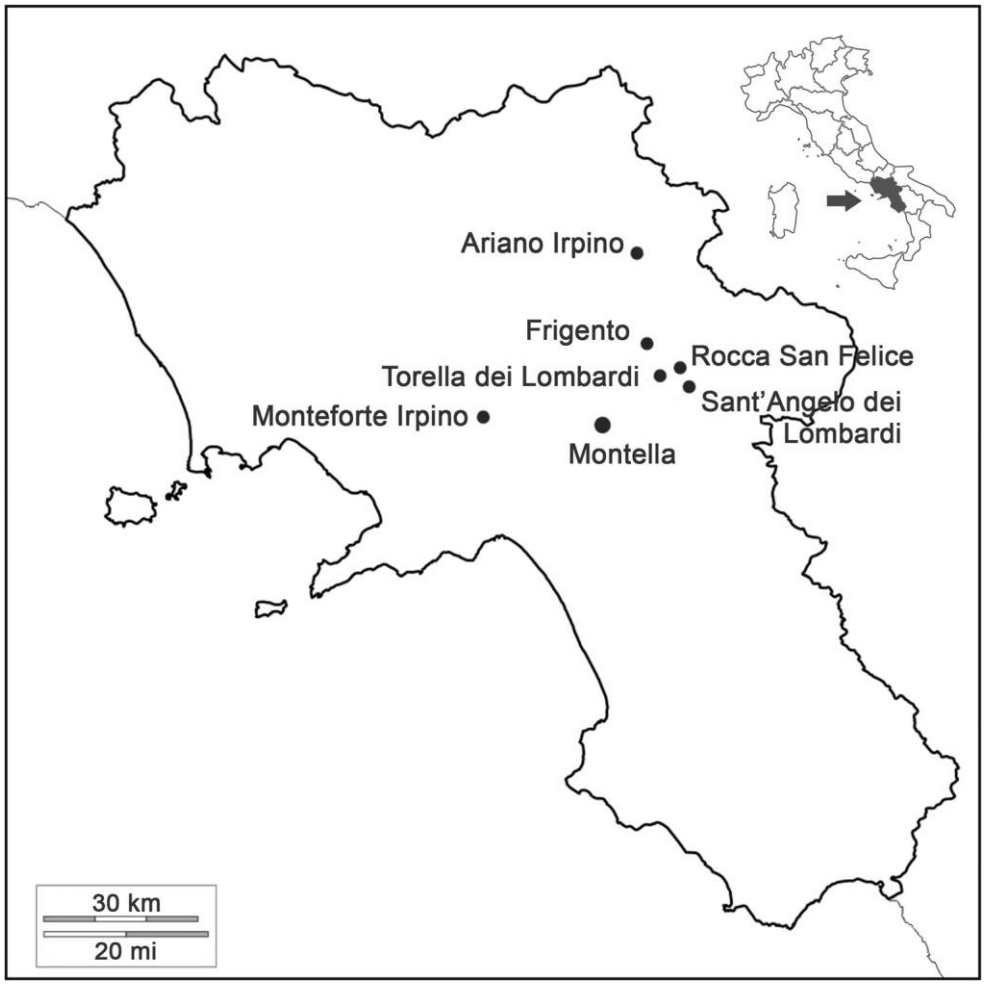

Fig. 1 Map of Campania highlighting the sites mentionedin this paper

The specific aims of this study are

- To define the technological characteristics of studied items;
- To identify production location/locations, more specifically to confirm the existence of a connection between the Apennine sites, as can be hypothesised due to the morphological and decorative similarities between thirteenth- and fourteenth-century products from Montella and those of the other Irpinian centres;
- To prove the archaeological hypothesis that *protomajolica*, transition enamel pottery and white enamel pottery are the result of technological evolutions in the field of glazed ceramic production.

Experiment

Materials

The finds of *protomajolica* and transition enamel pottery include morphologically homogeneous, mainly open shapes (bowls and plates), along with closed shapes (bottles and pitchers), which were used mainly in high socioeconomic contexts such as a court residence or hunting preserve. Stylistically, the collection of manufactured items is quite homogeneous; the glaze, when present, completely covers the internal surface of the open shapes and both surfaces of the closed ones.

Decoration motifs are principally taken from zoomorphic, plant, geometric and heraldic repertoires, which are a particular aspect of productions from Irpinia. The geometric decoration, which is more common, becomes simpler passing from protomajolica to so-called transition enamel pottery: on the former (Rotili 2011a), geometric motifs seem to be more creative and extemporaneous, and on the latter, decorations become more standardised and less depending on artisan extemporaneous creativity (Rotili 1999, 2011b). The presence of plant motifs (mainly on *protomajolica*) links the Montella settlement with many different social contexts in southern Italy, especially the Apulian areas. White enamel pottery is generally dated to the beginning of sixteenth century AD and is considered to be the common tableware used by the middle classes. There are a repertoire of standard shapes, bothopen and closed (plates, cups, basins, bottles and pitchers), and decorative motifs are no longer present. This type of vessel production was a great success, and it would go on until the emergence of pre-industrial pottery. The investigated shards—33 *protomajolica*, 18 transition enamel and 10 white enamelpottery—were coded as reported in Table 1, according to theirarchaeological classification. Figure 2 reports the examples representative of *protomajolica*, transition enamel and whiteenamel pottery from Montella.

It is important to underline that an autoptic examination of the objects revealed that the green hue of some *protomajolica* fragments (B6a and B6b—petroleum blue) differs from all the others.

Methods

Different interlocking techniques, involving both structural obervations and chemical-mineralogical analyses, were employed to examine the fragments, which are polarised-light optical microscopy (OM), scanning electron microscopy (SEM) with energy-dispersive spectrometry (EDS), X-ray powder diffraction (XRPD), inductively coupled plasma–mass spectrometry (ICP-MS) and laser ablation–inductively coupled plasma–mass spectrometry (LA-ICP-MS). Furthermore, the compositional data of the ceramic bodies were treated with multivariatestatistical techniques, carried out on standardised data using thesoftware package Minitab®.

For the ceramic body study, thin sections polished with a 3-μm diamond paste were subjected to orthoscopic polarised light observations with an optical microscope (Axioscop 40, Carl Zeiss) in order to examine the petrographic textures. The same thin sections were investigated by SEM using an EVO-50XVP, LEO; microanalyses were achieved with an X-max (80 mm^2) silicon drift Oxford detector supplied with a Super Atmosphere Thin Window ©. Powder X-ray diffraction analysis was performed employing a Philips X'Pert Pro X-ray diffractometer, with the following working conditions: CuKα Ni-filtered radiation, 40 kV and 40 mA of power supply, divergence slit 1°,anti-scatter slit 0.5°, receiving slit 0.2 mm and scan speed of 0.5°(2θ) per minute.

After the removal of the outermost layer that can have been contaminated during the burial, the ceramic body was scraped off, where existing fractures already damaged the fragments. In order to obtain the elemental chemical composition of the ceramic body, aliquots of 60 mg of the obtained ceramic bulk powder were dissolved by acid attack with a solution of 37% HCl, 70% HNO_3 and 40% HF (Fluka trace selected for trace analysis reagents) in a 1:4:5 (*v*/*v*/*v*) ratio and quantified by inductively coupled plasma–mass spectrometry (PerkinElmer Elan 9000 spectrometer). A standard clay material, the certified sample Brick clay ˆ standard reference materials 679 (National Bureau of Standards), was used to test the entire analytical procedure (analytical results and reference values for this brick clay were presented in Table A (in supplementary data)). External calibration with matrix-matching standards was employed for quantification, and three replicate readings were performed on both standards and samples (Mangone et al. 2008, 2009a, 2009b, 2013). Concerning the glazes and pigments, the cross sections of the samples were used, in order to investigate afresh, not weathered,surface, after polishing with a 3-μm diamond paste. ED X-raymicroanalyses were carried out with the silicon drift Oxford detector described above. It allows to detect the light elements even if their concentration is as low as 0.1%; in particular, the activearea of 80 mm^2 contributes to an effective detection of the elements that are near the detection limit for other ED detectors.Quantitative analyses were extracted from X-ray intensities using the algorithm of Pouchou and Pichoir (Pouchou and Pichoir 1988, 1991) supplied as software support by Oxford (UK).

Table 1 Bulk compositions by ICP-MS

Sample		Al_2O_3 (% *w*/*w*)	FeO	CaO	K_2O	MgO	TiO_2	Sr (ppm)	Cr	Ni
Green *protomajolica*	V1b	13.93	4.98	14.76	2.23	2.59	0.67	499	113	48
	V1c	15.06	5.32	12.19	3.05	2.65	0.72	433	108	46
	V2	14.79	5.59	12.17	2.80	2.55	0.70	487	116	48
	V3c	15.25	5.41	12.06	2.68	2.37	0.73	460	112	45
	V4	12.43	4.49	15.73	2.35	2.35	0.58	644	98	43
	V5	15.08	5.85	10.73	2.17	2.95	0.73	566	120	51
	V6	14.27	5.25	9.50	2.89	2.35	0.67	485	111	46
	V7a	14.91	5.48	12.91	2.47	2.49	0.70	502	110	53
	V7b	14.27	5.36	12.97	2.53	2.40	0.72	504	112	45
	V9	15.02	5.31	8.62	2.87	2.57	0.72	453	103	47
	V10	15.38	5.52	11.85	2.34	3.03	0.75	461	115	47
	V11b	14.74	5.34	11.89	3.08	2.75	0.70	443	112	47
	V11c	12.17	4.72	14.38	2.68	2.32	0.68	424	100	45
	V12	14.93	5.53	9.50	2.93	2.30	0.70	447	102	50
	V8a	14.49	5.16	9.53	2.75	2.40	0.70	401	99	40
	V8b	14.36	5.11	10.42	2.75	2.32	0.70	386	103	39
	V8e	12.89	4.85	12.03	2.69	2.34	0.62	382	88	33
Blue *protomajolica*	B1a	14.83	5.39	10.89	2.60	2.84	0.72	452	106	47
	B1b	14.44	5.32	14.03	2.88	2.42	0.72	417	108	44
	B2	16.36	5.45	11.82	2.54	2.87	0.68	553	110	57
	B3a	14.57	5.79	11.89	2.63	2.69	0.67	459	110	47
	B3b	15.12	5.47	9.64	2.75	2.80	0.68	414	109	47
	B4b	14.79	5.21	8.95	2.74	2.52	0.67	458	110	47
	B7	14.91	4.95	10.56	2.32	2.65	0.63	486	124	52
	B9	15.49	5.13	10.47	2.64	2.65	0.67	466	112	51
	B10	15.40	5.08	12.56	2.39	2.29	0.63	398	96	41
	B11a	13.85	4.75	13.14	2.42	2.45	0.63	450	104	44
	B11b	13.94	4.64	12.66	2.27	2.42	0.58	470	110	46
	B12	13.87	4.59	11.61	2.32	2.35	0.60	462	108	47
	B13a	13.70	4.75	10.62	2.26	2.49	0.60	492	104	47
	B13b	13.15	4.68	12.90	2.33	2.39	0.57	465	105	45
	B6a	11.62	3.96	10.05	2.23	1.94	0.55	431	88	33
	B6b	11.73	4.95	11.12	2.51	2.57	0.55	335	94	43
*		7.68 ± 0.48	4.04 ± 0.29	8.45 ± 1.26	2.15 ± 0.22	1.54 ± 0.12	0.40 ± 0.03	473 ± 50	108 ± 6	47 ± 3
Transition enamel	S1	11.85	5.57	8.83	2.02	2.67	0.68	353	105	45

Table 1 (continued)

Sample		Al_2O_3 (% *w*/*w*)	FeO	CaO	K_2O	MgO	TiO_2	Sr (ppm)	Cr	Ni
	S2	8.82	5.08	9.14	2.38	2.35	0.68	322	108	45
	S3a	16.57	5.71	7.44	2.64	2.69	0.73	386	134	51
	S3b	9.11	5.09	12.84	2.40	2.17	0.68	331	104	43
	S4	5.80	4.19	10.37	2.35	1.34	0.67	248	97	45
	S5a	6.80	4.94	9.71	2.24	1.76	0.73	267	105	48
	S5b	7.67	5.07	8.27	2.28	1.53	0.67	271	105	48
	S6a	10.86	5.25	7.51	2.38	2.39	0.70	338	122	45
	S6b	7.60	4.60	10.33	2.27	1.77	0.67	298	105	38
	S7a	10.22	5.52	8.09	2.36	2.60	0.67	438	112	47
	S7b	9.07	5.11	8.17	2.53	2.02	0.68	374	108	43
	S8a	4.84	4.21	7.58	1.96	1.23	0.70	231	95	46
	S8b	4.57	3.37	6.67	2.10	1.38	0.62	308	99	45
	S9a	10.51	5.61	8.33	2.46	2.87	0.67	439	113	47
	S9b	7.67	4.55	11.24	2.52	1.91	0.63	332	104	44
	S10c	10.39	5.26	15.74	2.47	2.74	0.70	366	110	45
	S10d	8.29	5.12	12.66	2.41	1.77	0.70	283	116	46
	S10e	10.09	5.16	10.33	2.02	2.80	0.63	441	111	47
*		4.73 ± 1.48	3.86 ± 0.46	6.88 ± 1.66	1.93 ± 0.16	1.27 ± 0.33	0.41 ± 0.02	335 ± 64	108 ± 9	45 ± 3
White enamel	Sa1a	24.85	7.90	9.47	3.73	3.88	1.08	619	150	36
	Sa1b	24.56	5.36	9.77	3.47	2.70	0.73	415	95	25
	Sa2a	17.19	5.27	9.86	3.04	2.57	0.73	515	104	48
	Sa3a	18.61	5.66	9.08	3.16	2.59	0.75	546	96	48
	Sa3c	16.53	5.40	9.85	4.42	2.44	0.75	393	87	44
	Sa4a	18.63	5.81	9.02	4.45	2.70	0.82	382	96	41
	Sa4b	17.48	5.39	9.81	4.06	2.57	0.77	404	89	38
	Sa5a	18.04	5.75	9.05	3.07	2.69	0.80	378	91	45
	Sa6c	17.40	5.66	9.56	4.06	2.24	0.75	430	94	46
	Sa7	17.93	5.98	9.07	2.87	2.54	0.82	393	90	46
*		9.38 ± 0.38	4.37 ± 0.19	6.72 ± 0.28	3.03 ± 0.56	1.53 ± 0.09	0.46 ± 0.02	430 ± 64	93 ± 5	44 ± 4

* Average chemical composition and standard deviation for each group, without outliers

Fig. 2 Finds from Montella. a *Protomajolica* with *blue* and *brown* decoration motifs. b *Protomajolica* with *green* and *brown* decoration motifs. c *Protomajolica* with *blue*, *green* and *brown* decoration motifs. d Transition enamel pottery. e White enamel pottery

The quantitative calibration of the silicon drift detector was possiblethanks to the analysis of natural standards on pure elementsmanufactured by Micro-Analysis Consultants Ltd. (UK). Analytical precision was 0.5% for concentrations >15 wt.%, 1% for concentrations of about 5 wt.% and <15% for concentrations near the detection limit. Given the analysed composition,the 1σ precision corresponded to the following values: SiO_2 = 0.10–0.20 wt.%, TiO_2 = 0.08–0.10 wt.%, Al_2O_3 = 0.08–0.13 wt.%, FeO = 0.05–0.15 wt.%, MnO = 0.04–0.6 wt.%, MgO = 0.08–0.13 wt.%, CaO = 0.04–0.14 wt.%, K_2O = 0.04–0.12 wt.% and Na_2O = 0.04–0.06 wt.%.

Two of the standards used for element calibrations (augite and orthoclase) are reported in Table B (in supplementary data).

When SEM-EDX was not sufficient to obtain satisfactory answers concerning the identification of the colouring pigments, LA-ICP-MS was used. It was the case of the blue areas in the lead glaze, where Co, due to its high colouring power, is generally present in amount below the detection limits of the EDS technique (0.05 wt%). The experimental conditions of ablation were optimised using standard lead glass materials, BCR-126A (Institute for Reference Materials and Measurements (IRMM)).

Results

Ceramic body: chemical and mineralogical analyses and statistical treatment of compositional data

In Table 1, the chemical composition of the ceramic bodies of all the fragments is reported.

The chemical data were treated with principal component analysis with the main aim of discriminating groups of objects on the basis of the compositional data, according to the archaeological category (Bruno et al. 1994; Catalano et al. 2007), provenance (Mirti et al. 2004; Mangone et al. 2009a, 2011; Giannossa et al. 2014a, 2016) or manufacturing process (Giannossa et al. 2014b, 2015; Mangone et al. 2008, 2009b, 2013). The diagram of the scores and loadings in the subspace of the first three principal components highlights different nuclei of sample aggregation per ceramic class (Fig. 3).

On the same samples, the results of the minero-petrographic investigations show a substantial similarity for all the ceramic bodies, evidence that very similar raw materials were used in their manufacture. There are only slight differences between objects belonging to the different ceramic classes, which are well-sintered ceramic body, medium-fine-grained (coarse silt) clay matrix with clasts mainly of quartzs (also volcanic ipo-ialin), feldspars, micas and ferruginous aggregates (also as pisolites) and pyroxenes (euhedral habitus) as accessories phases. Secondary calcite was commonly foundwithin the pores of most samples. Statistical treatment was carried out separately for each distinct group in order to high- light even the smallest differences between objects, which are minimised when the statistical treatment is extended to all classes.

Protomajolica

The diagram showing the scores and loadings of the first three principal components for samples of this class (Fig. 4) shows an enlarged group of objects, from which samples B6a, B6b,V8a, V8b and V8e differ. The chemical indiscrimination between blue and green *protomajolicas*, which suggests that the same raw materials were used, can be explained by assuming that most of the analysed samples, featuring only blue and green decoration, might actually belong to the same blue andgreen object.

For the samples B6a, B6b,V8a, V8b and V8e, a minero-petrographic diversity is also highlighted by OM and SEM-EDS. The ceramic bodies of samples B6a and B6b (Fig. 5) are richer in quartz and K-feldspars (due to the larger amounts of sand fraction) and are consequently poorer in clayey matrix, whilst the bodies of the ceramic samples V8a, V8b and V8e, besides having a primary porosity complex geometry, belong to a different mineralogical/petrographic class (e.g. larger amounts of quartz and smaller quantities of feldspars, finer grain size).

Transition enamel pottery

The results of the multivariate treatment for this ceramic class show the formation of a single group remarkably spread along PC1. OM and SEM-EDS analyses revealed no differences

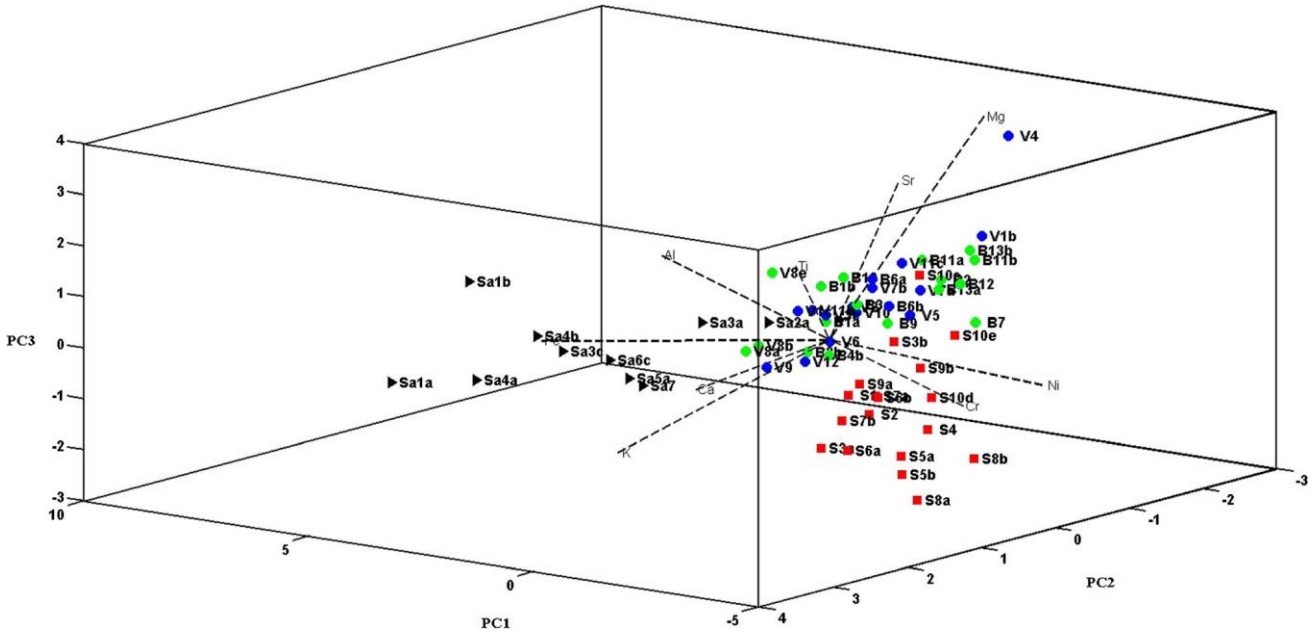

Fig. 3 Scores and loadings diagram for the first three principal components related to the ceramic bodies analysed, *blue protomajolica*(*blue circle*), *green protomajolica* (*green circle*), transition enamel pottery (*red square*) and white enamel pottery (*black triangle*). The accounted variance is 79% of the total variance

between the samples from this cluster with the exception of sample S10c, in which some relatively big clasts (fine sand) of calcite can be seen. Their presence, along with the good level of sinterisation, suggests that a raw material coarser than that of samples belonging to the same class was used and calcite clasts did not complete their decomposition reaction due to their larger dimension (Fig. 5). This explains why chemical analysis revealed a higher amount of Ca in this sample than other samples from the same class. It can be hypothesised that this coarser raw material used for sample S10c may be the same used for all other samples belonging to the same class but taken from a different area or sedimentary level, as will be explained in detail later in the paper. It is interesting to underline that in transition enamel ceramic bodies, pyroxenes greater than 100 μm (Fig. 6) are more frequently found in transition enamel ceramic bodies than in other classes of pottery.

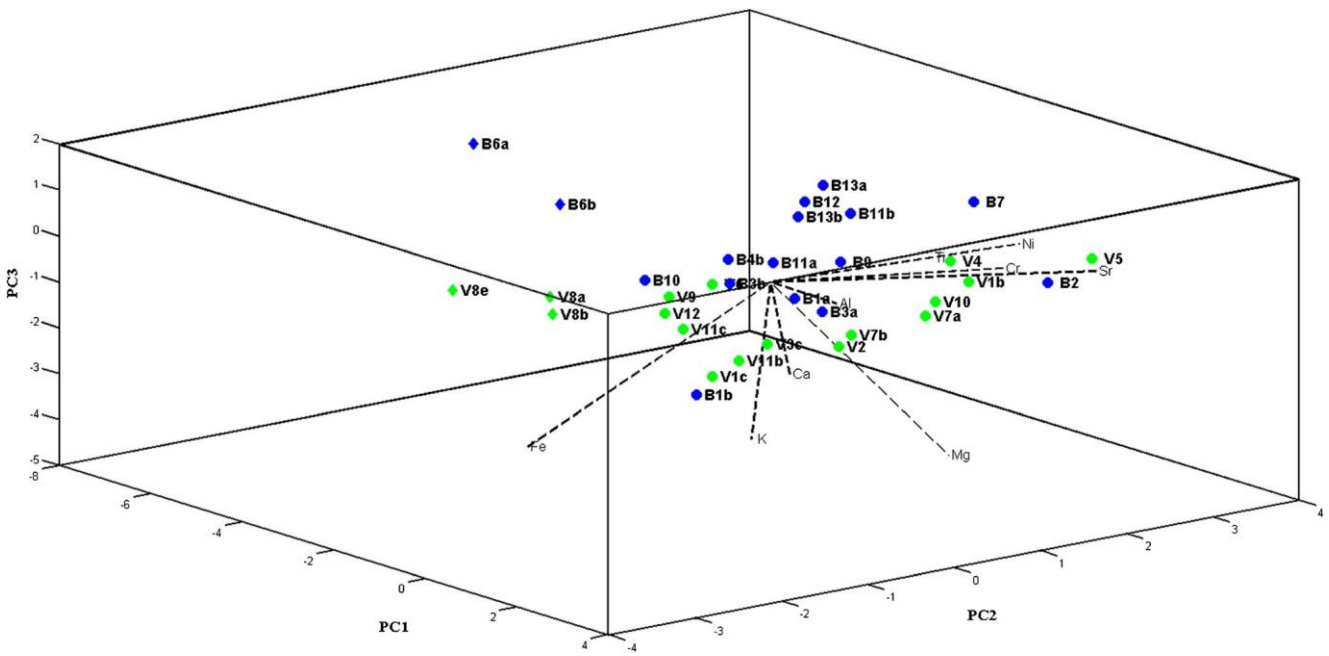

Fig. 4 Scores and loadings diagram for the first three principal components. The accounted variance is 82% of the total variance

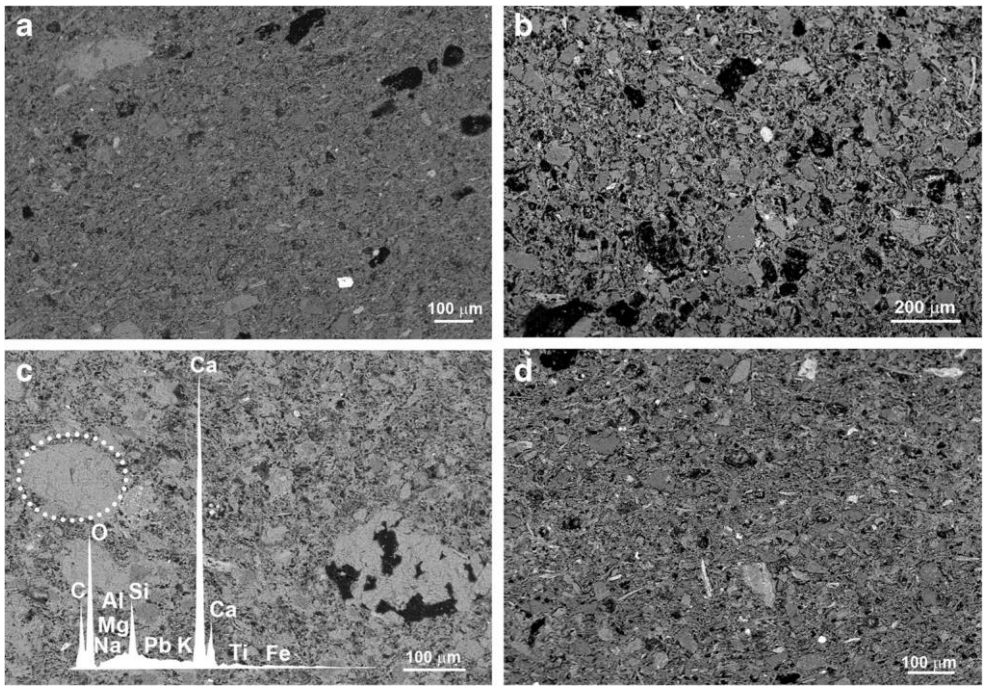

Fig. 5 SEM-BSE photomicrographs of thin sectionsof some fragments, showing the different characteristics of their ceramic bodies: V10 (a), B6a (b)—rich in quartz and K- feldspars and poorer in clayey matrix, S10c (c)—rich in calcite clasts (brighter) and Sa1a (d)— rich in mica crystals

White enamel

The scores and loading diagram of the first three principal components are shown in Fig. 7. All the objects, with the exception of samples Sa1a and Sa1b, are grouped into a single cluster.

The outlier position of the ceramic body of samples Sa1aand Sa1b in the PCA diagram is supported by their different minero-petrographic composition (Fig. 5d). Along with the minerals commonly identified in all the pottery classes, fragments of igneous rocks and many biotite crystals in which titanium—even if only in trace amounts—is present can be identified in their ceramic bodies. This group's samples, whose composition is particularly homogeneous, show the highest Al and Fe concentrations linked to the presence of alarge amount of Fe oxide aggregates (also as pisolites)(Fig. 5d).

Diffraction data for all the ceramic classes (Table 2) show a perfect correspondence with the data obtained from microscopy investigations on the thin sections. The range of equivalent firing temperatures (EFTs) for the samples analysed by XRPD was estimated according tothe thermal stability ranges (appearance/disappearance of given phases) determined by experimental firings of Ca- rich clays found in recent literature (Maggetti 1982; Riccardi et al. 1999; Cultrone et al. 2001; Maritan et al. 2006; Maggetti et al. 2011; Eramo et al. 2014). The pres- ence of neo-formed phase gehlenite and pyroxenes in all samples (in different relative quantities) suggests that their ceramic bodies reached a temperature of 900–1000 °C, a temperature which was maintained for at least long enough to complete the reaction between clayey minerals and calcite during the firing process (Eramo et al. 2014). This did not occur with all samples; indeed, an almost com-plete destruction of clay minerals is not associated with a complete destruction of carbonates (also due to the differentparticle sizes). Therefore, the neoformation process of high-temperature crystals could not be fully carried out.

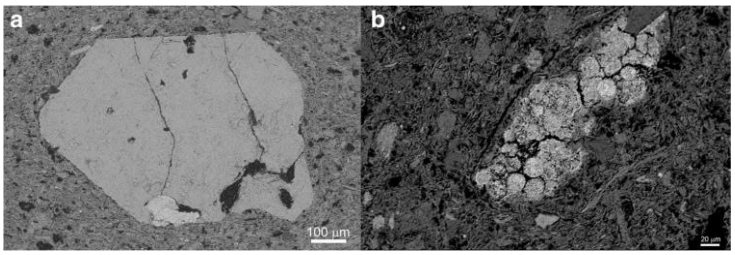

Fig. 6 SEM-BSE photomicrographs of the thin section of samples S9b (a), showing a pyroxene (euhedral habitus) in the ceramic body, andSa1a (b), showing a Fe-oxide pysolite present in the ceramic body

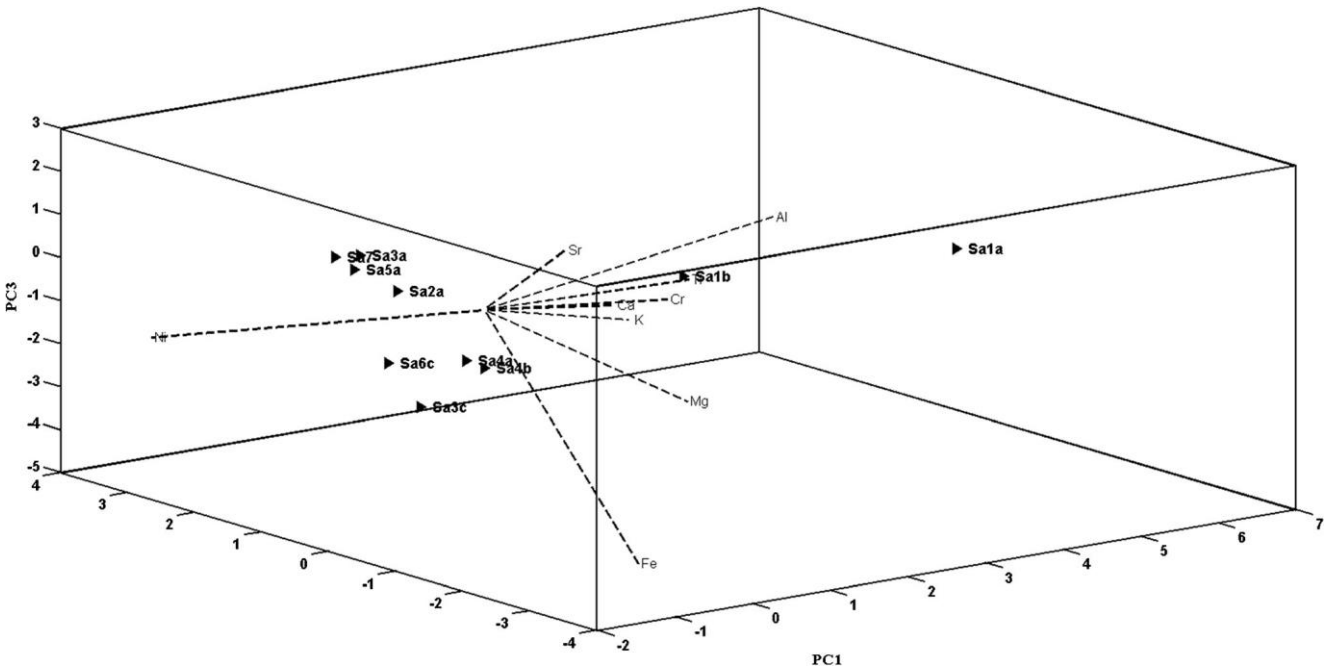

Fig. 7 Scores and loadings diagram for the first three principal components. The accounted variance is 81% of the total variance

Table 2 Mineralogical composition, by PXRD analysis, of some representative samples

Sample	*Mic*	*Qtz*	*Fld*	*Cal*	*Px*	*Gh*	*Hem*
B6b	/	XXXXX	XXX	X	XX	XX	/
B13a	/	XXXXX	XXX	/	XXX	XX	X
B1b	X	XXXXX	XXX	XX	XX	XX	X
B12	/	XXXXX	XXX	X	XXX	XX	X
V3b	/	XXXXX	XXX	/	XXX	/	tr
V7a	/	XXXXX	XX	/	XXX	X	tr
V8e	/	XXXXX	XX	X	XX	XX	tr
V2	/	XXXXX	XXX	XX	XX	XXX	tr
V8b	/	XXXXX	XX	X	XX	XX	X
S9a	tr	XXXXX	XXX	X	XX	XX	tr
S9b	tr	XXXXX	XXX	XX	XXX	XX	tr
S2	tr	XXXXX	XXX	XX	XXX	XX	tr
S7a	tr	XXXXX	XXX	XX	XX	X	tr
S10c	/	XXXXX	XXX	X	XXX	X	tr
Sa3a	/	XXXX	XXX	X	XXX	tr	/
Sa3c	/	XXXXX	XXX	XX	XXX	XX	X
Sa5a	tr	XXXXX	XXX	X	XX	XX	X
Sa6c	/	XXXXX	XXX	XX	XX	XXX	X
Sa7	/	XXXX	XX	/	XX	X	tr
Sa1a	tr	XXXXX	XXX	Tr	XXX	XX	tr
Sa1b	/	XXXXX	XXX	Tr	XXX	tr	tr
Sa2a	/	XXXXX	XXX	XX	XXX	tr	tr
Sa4a	X	XXXXX	XXX	X	XX	XX	tr

Mineral abbreviations (Kretz 1983) *Mic* micas, *Qtz* quartz, *Fld* K-feldsparand plagioclase, *Cal* calcite, *Px* pyroxene (diopside), *Gh* gehlenite, *Hem* hematite. Scale of relative abundance *XXXXX* very abundant, *XXXX* abundant, *XXX* good, *XX* present, *X* scarce, *tr* traces. / absent

Glazes: chemical and structural analyses

The covering is tin-opacified lead glaze for all the ceramic classes. Tin oxide, formed during the dissolution and recrystallisation of SnO_2 in the $PbO–SiO_2$ melt (Molera et al. 1999), is present as fine dispersed particles, typically less than 3 μm. Inside the glaze crystal wrecks, mostly alkali feld-spars but also quartz and spheroidal vesicles (Fig. 8a), can beseen. Passing from *protomajolica* to transition enamel to white enamel, the thickness of the glazed coating gradually in- creases (60–150 > 220 > 350 μm), whilst the amount and dimension of crystals wrecks decrease (up to 100 μm for *protomajolica*, lower than 20 μm for white enamel).

The firing process was obtained in one step, as can be inferred from the non-sharp contact between the glaze and the ceramic body, from the presence of a thick layer of interface which is rich in newly formed crystals of K and Pb feldspars of characteristic and constant composition (Fig. 8b, small letter o) and from the Pb penetration in the ceramic body. The three classes have a layer in common (of different compositions) in the upper part of the ceramic body; its function is to lighten the colour of the ceramic body surface.

In the case of *protomajolica* and transition enamel, this layer is Mg based. The presence in the lower part of the glaze of newly formed crystals based on Si, Mg, Ca, Pb and Fe is due to this (Fig. 8b, asterisk). These crystals might have formed due to the reaction between the forming glaze and Mg-based crystals—probably micas—gathered in the upper area of the ceramic body for some tens of microns of thick-ness. It seems that the opalescence of the coatings is due to the presence of these minerals below the glaze (Vendrell et al.

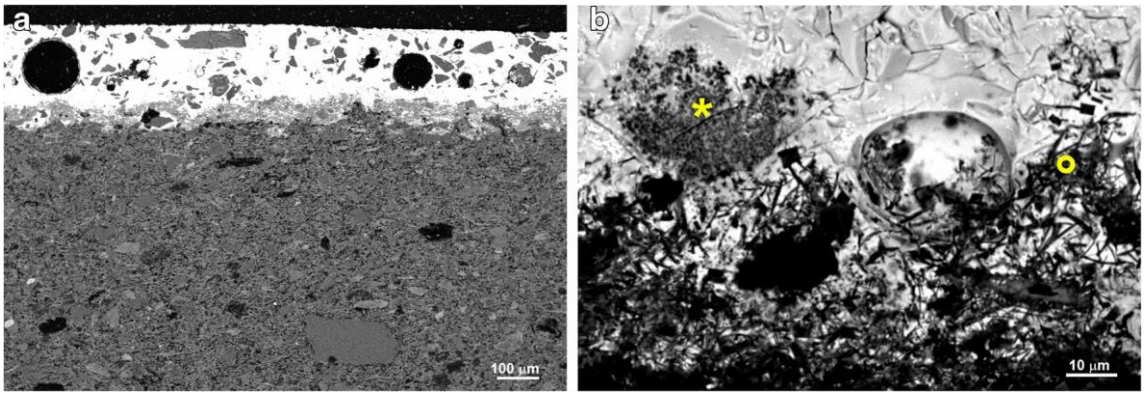

Fig. 8 a SEM-BSE photomicrograph of the thin section of sample B13b which shows, from *top to bottom*, the tin-opacified lead glaze with wreckcrystals of quartz, alkali feldspars and spheroidal vesicles, the interfacelayer and the ceramic body. b SEM-BSE photomicrograph of sample V10 pseudo-arborescent structures rich in Mg (*asterisk*) and newly formed Kand Pb feldspars (*small letter o*) are visible. In the *upper part* of the glaze,Sn compound aggregates can be seen as brighter spots

2000; Mason and Tite 1997); their ivory-greyish colour is caused by a relatively high iron content (Swann et al. 2000).This kind of under-glaze layer had already been observed in the Apulian *protomajolica* shards found in the castle of Canosa (Apulia, Italy) (Mangone et al. 2009b). In the Middle Ages, an under-glaze layer was used as an alternativeto an opaque glaze, reducing the amount of tin required. Tinwas both expensive and difficult to find. However, in whiteenamel pottery, the presence of newly formed crystals of wollastonite (Fig. 9b, cross) and of silicates based on Al, Pb, Ca,Na and K (Fig. 9b, small letter o) or on Al, Ca, Mg and Fe (Fig. 9b, asterisk) in the interface area glaze-ceramic body suggests that lime was employed on the ceramic body surface.

As concerns firing and raw materials, the presence of a small but constant quantity of Sb (about 0.5%, as measured by EDS) in the glaze of transition enamel pottery suggests that a different source of raw materials to that employed in protomajolica and white enamel pottery was used to introduce Pb or Sn. This hypothesis is also supported by the presence, in the glazes of this class, of zoned feldspar crystals—probably of high-temperature volcanic origin. These feldspars (Table 3 spot 1 and Fig. 10) often reacted with the Pb-rich molten glaze to re-equilibrate their chemical composition or to form new phases. In particular, the presence of some zoned sanidine with a Ca-rich rim can be highlighted. In the coronitic position, against the Ca-rich rim of this sanidine, very few euhedral Na–K–Pb silicatic phases grew (Table 3 spot 8 and Fig. 10) with a sanidine-like crystal chemical formula. Furthermore, the Na–Ca-rich sanidine rim reacted with the molten glaze and largely changed its composition with the capture of Pb (Table 3 spots 6 and 7). The Pb spread into the whole crystal penetrating through the fractures and also reached the inner zone of the sanidine (Table 3 spots 2–5 and Fig. 11).

This leads us to believe that higher firing temperatures and longer firing times were employed than in the production of *protomajolica*. This theory is also supported by the presence

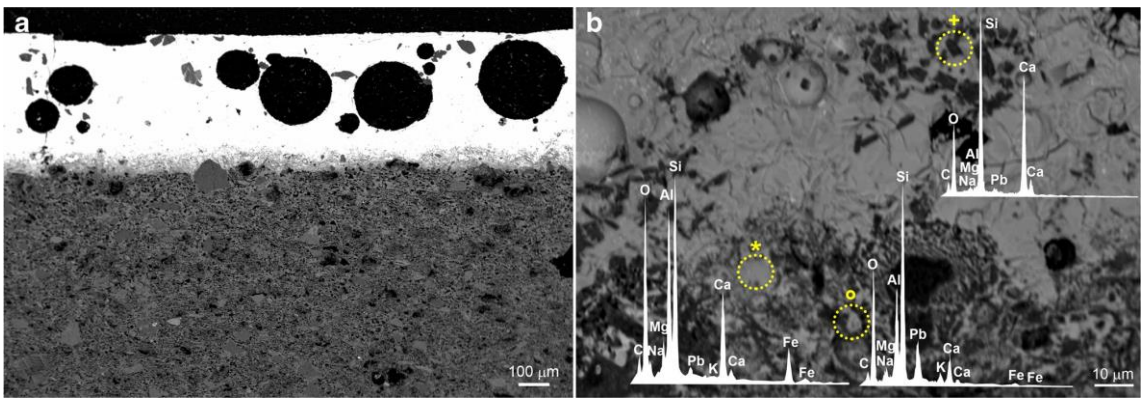

Fig. 9 a SEM-BSE photomicrograph of the thin section of sample Sa2awhich shows, from *top to bottom*, the lead-stanniferous glazed coating,the interface layer and the ceramic body. b SEM-BSE image of newly formed crystals in the glaze-body interface of Sa2a sample. Euhedral wollastonite crystals (*cross*); crystals based on Al, Ca, Mg and Fe (*asterisk*); and on Al, Pb, Ca, Na and K (*small letter o*)

Table 3 Microanalyses by EDS of a zoned sanidine and of a neomorphic Na–K–Pb silicatic phases (formula on the basis of eight oxygens) in coronitic position present in the glaze of sample S5b

Spot		Composition						Formula						
		SiO_2 (*w*/*w*%)	Al_2O_3	PbO	CaO	Na_2O	K_2O	Si	Al	Pb	Ca	Na	K	Σcat.
Core	1	64.95	18.57	0.00	0.44	1.62	14.43	2.99	1.01	0.00	0.02	0.14	0.85	5.01
	2	62.97	17.91	2.08	0.75	1.31	14.97	2.97	0.99	0.03	0.04	0.12	0.90	5.05
	3	61.79	17.97	3.74	0.86	1.25	14.39	2.95	1.01	0.05	0.04	0.12	0.88	5.05
	4	61.96	17.86	5.00	0.62	1.37	13.19	2.96	1.01	0.06	0.03	0.13	0.80	4.99
	5	60.92	17.70	5.70	0.99	1.24	13.46	2.94	1.01	0.07	0.05	0.12	0.83	5.02
Rim	6	33.89	23.63	36.94	2.74	0.69	2.11	2.18	1.79	0.64	0.19	0.09	0.17	5.06
	7	33.81	23.82	37.01	2.41	0.82	2.13	2.17	1.81	0.64	0.17	0.10	0.17	5.06
Corona	8	57.77	13.08	16.28	0.80	0.71	11.38	3.04	0.81	0.23	0.05	0.07	0.76	4.96

of SnO_2 particles in the recrystallisation phase with the formation of acicular structures (spatial distribution that looks likethe Widmanstätten pattern (Burke 1986) (inset in Fig. 10)). The formation of SnO_2 crystals with the same morphology isalso due to extremely high firing temperatures (up to 1100 °C)followed by a relatively high cooling speed, as evidenced by experiments simulating the formation of glaze (Molera et al.1999). Moreover, the better homogeneity of the glaze and thelower amount of crystal wrecks indicate a more accurate process of glaze preparation and, as a result, a quicker and moreefficient process of fusion and anchoring of the glaze itself tothe ceramic body.

Regarding the pigmented areas, the widespread presence of Cu, sometimes associated with Fe, in the green areas and Fe plus Mn in the brown areas is revealed by both EDS and LA-ICP-MS results. Co in the blue areas is revealed by LA-ICP-MS results. The presence of Mn seems to be connected to the morphologic variations of the glaze-body interface layer, which appears like a densely packed layer of neo-formed crystals (Fig. 12a).

Besides differing in microstructure, the three glaze classes differ also in their composition, as highlighted by the analysis carried out by EDS (De Benedetto et al. 2004; Gulmini et al. 2006, 2015) on 21 samples (6 *protomajolica*, 8 transition enamel and 7 white enamel), chosen from the most representative of the three classes. Due to the low solubility of tin oxide in glaze melts, the microanalyses were performed on a rastered area of the specimen whose side was at least 50 μm in length, in any case large enough to be representative of the mean composition of the glaze. During microanalyses of the glaze, particular attention was paid in order to avoid quartz, feldspar and other minerals present as wreck xenocrystals and spheroidal vesicles which are often present in the coating. Results are shown in Table 4, in which Sb, present as an impurity only in the transition enamel glazes, was excluded. The Pb amount is on average between 35 and 45% in PbO, and the alkali contents are down to around 3.5% (Na_2O + K_2O). The greatest difference between ceramic classes can be observed in the SnO_2/PbO ratio. Information concerning production technology cannot be inferred from SiO_2/PbO variability since the value of this ratio is conditioned by the fact that the measure was carried out excluding relict crystals (quartz plus feldspars), essential components in production itself.

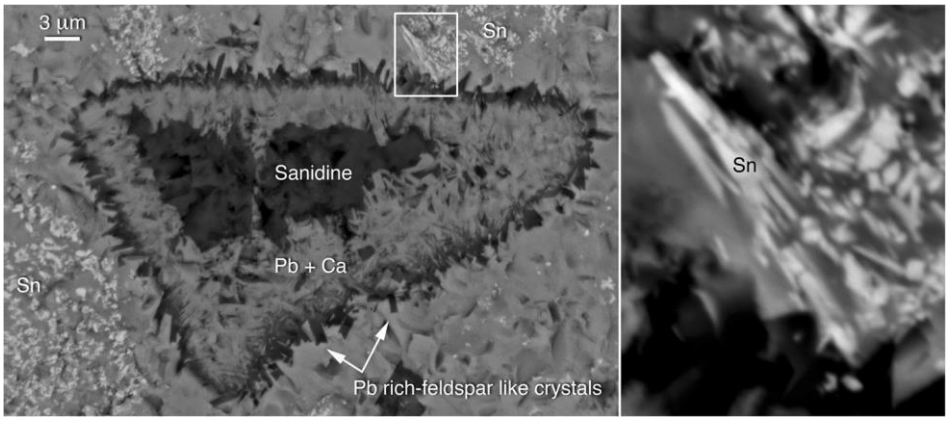

Fig. 10 SEM-BSE photomicrograph of the thin section of the sample S5b whichshows a high-temperature feldspar present in the glaze. *Inset* shows the SnO_2 particles showinga spatial distribution that sometimes looks like the Widmanstätten pattern (Burke 1986, Cosmic debris: meteorites in history, University of California Press, 1986)

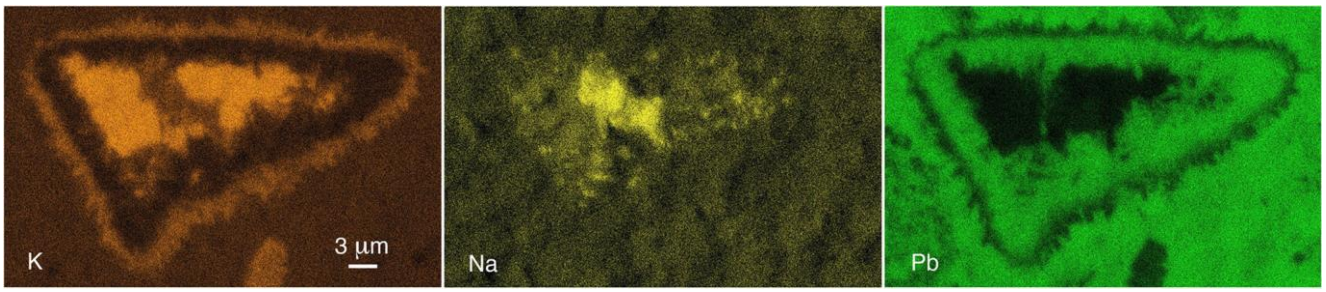

Fig. 11 SEM-EDS chemical maps of K, Na and Pb of the area reported inFig. 10: the increase of pixel intensity and density corresponds to an increase in the element concentration. In the maps it is evident that theoriginal composition of a natural K-Na feldspar, still present in the core, is instead transformed into a Pb-rich feldspar at its rim. Some little neomorphic and euhedral Pb-rich crystals developed in coronitic position at the rim of the K-Na feldspar in contact with the Pb-rich molten glaze

Regarding samples whose ceramic bodies are different fromthe others (B6a, B6b, V8a, V8b and V8e), features of the inter-face layer and of the glaze allow us to state that their diversitydoes not only concern the rather different materials used to makethe ceramic bodies but also the materials and the technology employed to create the glaze. The glaze on samples B6a and B6b, for instance, has a thickness which is definitely above the average—about 300 µm—with Sn present in big aggregates—irregular shapes—on its inside (Fig. 12b). This peculiarity maybe due to a bad grinding/mixing of the raw materials duringglaze preparation, which did not allow an adequate Sn spreadin the glaze. For the same samples, the strange hue of the blue colour, highlighted by a visual examination, is due to the choiceof a different colouring pigment, copper instead of cobalt, as highlighted by LA-ICP-MS results. As regards V8a, V8b and V8e, the MO and SEM analyses showed an engobe layer below the glaze and a sgraffio (Giannossa 2014b; De Benedetto et al. 2011) on V8a sample (Fig. 13). This leads us to conclude that these fragments belong to a different ceramic class.

Conclusions

The results obtained show that using a combined approach of analytical techniques, it is possible to identify the technology and raw materials used in the production of archaeological finds. The multivariate statistical treatment applied to the matrix of the ceramic bodies' compositional data obtained through chemical analysis proved to be an important instrument in the highlighting of similarities and differences between finds coming from the same archaeological site. On the other hand, the useof other analytical methods such us optical and scanning electron microscopies was essential in order to provide a completereconstruction of the production technology process and theidentification of when this process was carried out.

Regarding raw materials used in production, the different chemical and minero-petrographic features of the Montella samples; the blue-grey clays of the Irpinian area (Di Pierro and Moresi 1982, 1983; Dell'Anna and Laviano 1982, 1983; Balenzano and De Marco 1984); and, above all, the abundance of pyroxenes with an intact crystal habit without trans- port traces (edges smoothing), as is typical of short transport, and the presence of iron oxide pisolites, both absent in the clays, are all factors which lead us to believe that blue-greyclays were not used in the production of the ceramic bodies. Montella pottery does not even have chemical and minero-petrographic similarities with that of Ariano, a manufacturing centre with which Montella shares so many marked decorative and morphologic similarities that archaeologists hypothesised a common production (Rotili and Busino 2017). The chemical

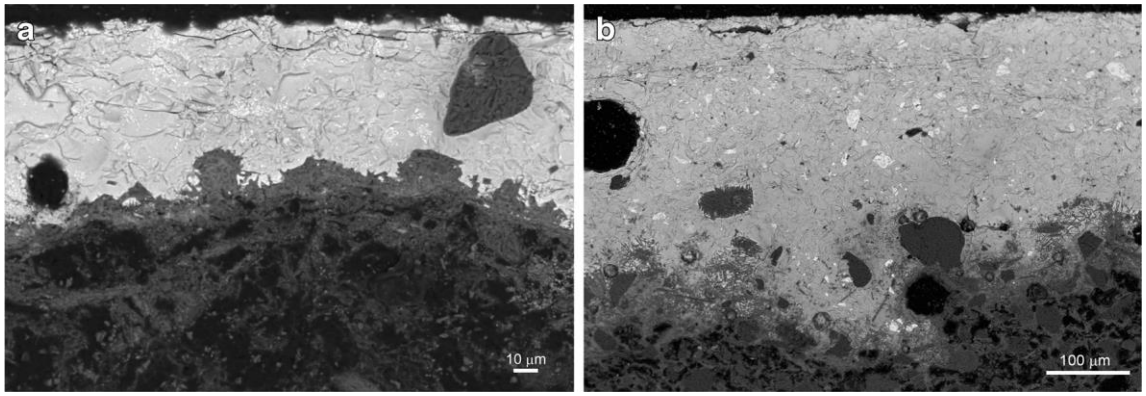

Fig. 12 SEM-BSD photomicrographs of the thin sections of samples V10 (a), which shows the glaze-body interface layer in the areas where Mn ispresent, and B6a (b), highlighting the thick vitreous coating with big Sn compounds (brighter)

Table 4 SEM-EDS microanalyses of the glaze of some representative samples of the three ceramic classes

Sample	(*w*/*w*%)																		
	Na_2O		MgO		Al_2O_3		SiO_2		K_2O		CaO		FeO		Sb_2O_3		SnO_2		PbO		SnO_2/PbO
	Mean	σ	Mean	σ	Mean	σ	Mean	σ	Mean	σ	Mean	σ	Mean	σ	Mean	σ	Mean	σ	Mean	σ	
V5	1.21	0.04	0.67	0.04	2.84	0.04	40.33	0.11	2.46	0.07	3.42	0.09	1.59	0.09	–		6.25	0.15	41.22	0.15	0.15
V12	0.36	0.06	0.41	0.04	3.28	0.04	31.91	0.10	0.86	0.07	3.26	0.09	0.90	0.09	–		7.98	0.15	51.03	0.18	0.16
B10	0.66	0.05	0.49	0.05	3.02	0.05	34.21	0.10	1.00	0.09	3.30	0.08	0.62	0.08	–		6.85	0.15	44.24	0.17	0.15
B13b	0.80	0.08	0.19	0.03	1.84	0.03	39.55	0.10	2.73	0.08	1.14	0.07	0.16	0.08	–		6.54	0.17	47.04	0.17	0.14
S6b	0.86	0.04	0.30	0.03	4.32	0.04	37.87	0.10	2.00	0.07	3.37	0.09	0.53	0.09	0.60	0.16	10.35	0.16	40.41	0.18	0.26
S1	1.47	0.05	0.69	0.04	6.21	0.05	39.58	0.13	2.39	0.08	5.02	0.10	1.26	0.10	0.40	0.17	7.80	0.17	35.58	0.18	0.22
S5a	0.79	0.08	0.37	0.07	2.97	0.08	34.51	0.15	2.25	0.09	2.30	0.14	0.97	0.15	0.50	0.15	13.27	0.18	42.58	0.19	0.31
S6b	1.03	0.04	0.45	0.03	4.92	0.04	40.49	0.10	2.25	0.07	1.86	0.10	1.09	0.10	0.58	0.16	8.27	0.14	39.64	0.17	0.21
S10c	0.76	0.07	0.54	0.05	5.39	0.06	40.68	0.11	2.04	0.08	4.79	0.09	1.36	0.12	0.48	0.18	10.22	0.14	34.23	0.17	0.30
Sa4c	0.60	0.06	0.30	0.03	4.05	0.04	39.69	0.10	2.03	0.07	2.76	0.14	0.67	0.09	–		17.29	0.19	32.60	0.16	0.53
Sa3c	0.49	0.05	0.39	0.04	4.03	0.04	31.94	0.10	1.49	0.10	2.85	0.10	0.96	0.09	–		17.71	0.17	40.13	0.16	0.44
Sa6c	0.76	0.06	0.32	0.03	4.19	0.05	38.31	0.11	2.5	0.06	2.86	0.09	0.58	0.08	–		12.77	0.17	37.71	0.17	0.34
Sa7	0.72	0.06	0.57	0.04	4.73	0.05	42.64	0.13	1.93	0.09	4.62	0.08	1.23	0.09	–		12.92	0.18	30.65	0.15	0.42

Each reported value is the mean of at least three microanalyses

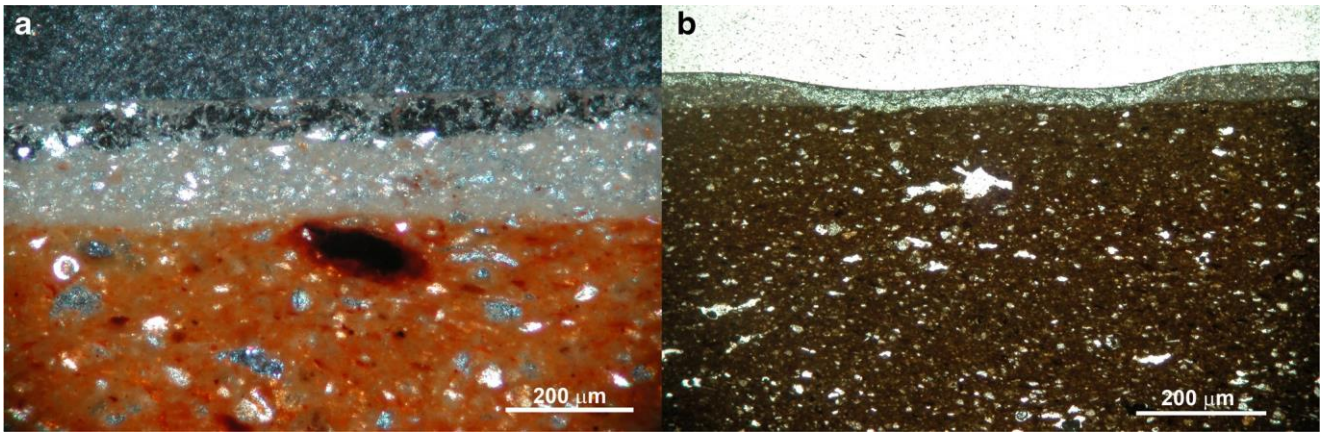

Fig. 13 MO photos of the thin section of fragment V8a, highlighting an engobe layer (crossed Nicol, a) and a sgraffio (polarised light, b) below the glaze

and minero-petrographic features of the ceramic bodies of the three studied classes suggest, however, the use of the same raw material, that is, the eluvial and fluvial-lacustrine deposits present in the area of Montella site (sheet 186 Sant'Angelo dei Lombardi, Geological Map of Italy). These deposits, characterised by minero-petrographic and granulometric variabilities, both in lateral and in vertical etheropies, are made of graveland silty-clayey sands and/or sandy-clayey silts, some- times mixed with reworked pyroclastic materials (pyroxens, igneous rock fragments, etc.) and are very similar, from a minero-petrographic and a genetic point of view to terre rosse (red earths, widely studied deposits of close areas (Dell'Anna 1967; Dell'Anna and Laviano 1991) present in sheet 186). Their use as raw materials, together with the differences highlighted in the production technology employed,fully explains the slight compositional variability of the ceramic bodies, such as the higher amounts of Al and Fe in thewhite enamel class due to the use of eluvial silt levels rich inresidual materials (red earth). Regarding the glazes used, different sources of raw materials were employed, as suggestedby the constantly small quantity of Sb found in the transitionenamel glazes alone. Also, dissimilarities in the technological process were noticed for the glazes of all three classes. For each of them, firing was carried out in one step, as witnessed by the non-sharp contact between the glaze and the ceramicbody, by the presence of the dense network of newly formed crystals and by the Pb penetration in the ceramic body; the reached temperatures were high, as demonstrated by the good sintering of the ceramic body and by the abundance of newlyformed hematite and gehlenite crystals. However, the firingduration was different for the three classes, shorter for the *protomajolica* than for the other two. Useful information for the reconstruction of the technological process and the identification of the materials used to make the glaze can be extract-ed from the analysis of the wreck crystals in the glaze itselfand from the different newly formed crystal at the interface.Indeed, the number and dimension of the wreck crystals in the glaze indicate that preparation and care in the grinding and sifting of the materials improved gradually passing from *protomajolica* up to white enamel. The different interface crystals indicate the application of a Mg-based layer for protomajolica and transition enamel and a Ca-based layer for white enamel, before the superposition of the glaze. Manufacture was optimised with time, as suggested by the morphological observation of the glaze that becomes thicker and more homogenous. The presence of ceramic body quartz crystals slotted in the glaze and the non-homogeneous penetration of glaze parts in the body—signs of an inaccurate polishing of the ceramic body—are characteristics of *protomajolica* alone. The composition of these glazes also seems to have changed over time as is evident from the Sn/Pb ratio. The results as a whole confirm the archaeological hypothesis, suggesting that transition enamel pottery is characterised by intermediate features between *protomajolica* and white enamel pottery.

Acknowledgements This work has been partially supported by the Project MAIND (PON 2007–2013 cod. PON03PE_00004_1).

References

Balenzano F, De Marco A (1984) Caratteri granulometrici, mineralogici e chimici ed aspetti paleoambientali delle Argille Azzurre di Guardia Lombardi (Av). Geologia Applicata e Idrogeologia Volume XIX, Bari

Bevere R (1940) I dacia della città di Ariano. Samnium 13:31–43

Bruno P, Caselli M, Curri ML, Favia P, Laganara C, Lamendola R, Mangone A, Traini A (1994) XPS, ICP and DPASV analysis of medieval pottery. Statistical multivariate treatment of data Fresenius J Anal Chem 350:168–177

Burke JG (1986) Cosmic debris: meteorites in history. University of California Press, 1986.

Catalano IM, Genga A, Laganara C, Laviano R, Mangone A, Marano D, Traini A (2007) Lapis lazuli usage for blue decoration of polychrome painted glazed pottery: a recurrent technology during the middle ages in Apulia (southern Italy). J Archaeol Sci 34 (4:503–511

Cultrone G, Rodriguez-Navarro C, Sebastián E, Cazalla O, de la Torre MJ (2001) Carbonate and silicate phase reactions during ceramic firing. Eur J Mineral 13:621–634

De Benedetto GE, Acquafredda P, Masieri M, Quarta G, Sabbatini L, Walton M, Tite M (2004) Investigation on Roman lead glaze from Canosa: results of chemical analyses. Archaeometry 46(4):615–624

De Benedetto GE, Nicoli S, Pennetta A, Rizzo D, Sabbatini L, Mangone A (2011) An integrated spectroscopic approach to investigate pigments and engobes on pre-Roman pottery. J Raman Spectrosc 42: 1317–1323

Dell'Anna L (1967) Ricerche su alcune terre rosse della regione pugliese. Periodico di Mineralogia 36(2):539–592

Dell'Anna L, Laviano R (1982-1983) Composizione mineralogica, granulometrica e chimica delle Argille Grigio-Azzurre inframesoplioceniche di Cairano e Conza della Campania (AV). Rendiconti Società Italiana di Mineralogia e Petrologia 38(2):871–881

Dell'Anna L, Laviano R (1991) Mineralogical and chemical classification of Pleistocene clays from the Lucanian basin (southern Italy) for the use in the Italian tile industry. Appl Clay Sci 6:233–243

Di Pierro M, Moresi M (1982-1983) Caratteri granulometrici, mineralogici e chimici dei sedimenti pelitici infra-mesoplioceniciici di Calitri e S. Andrea Di Conza (AV). Rendiconti Società Italiana di Mineralogia e Petrologia 38(1):353–366

Eramo G, Giannossa LC, Rocco A, Mangone A, Graziano SF, Laviano R (2014) Oil lamps from the catacombs of Canosa (Apulia, fourth to sixth centuries AD): technological features and typological imitation. Archaeometry 56:375–391

Giannossa LC, Acquaviva M, De Benedetto GE, Acquafredda P, Laviano R, Mangone A (2014a) Methodology of a combined approach: analytical techniques to identify technology and raw materials of thin walled pottery from Herculaneum and Pompeii. Anal Methods 6(10):3490–3499

Giannossa LC, Acquaviva M, Laganara C, Laviano R, Mangone A (2014b) Applications of a synergic analytical strategy to figure out technologies in medieval glazed pottery with ʙnegative decoration^ from Italy. Appl Phys A Mater Sci Process 116(4):1541–1552

Giannossa LC, Fico D, Pennetta A, Mangone A, Laviano R, De Benedetto GE (2015) Integrated investigations for the characterisation of Roman lead-glazed pottery from Pompeii and Herculaneum (Italy). Chem Pap 69(8):1033–1043

Giannossa LC, Mininni RM, Laviano R, Mastrorocco F, Mangone A, Caggiani MC (2016) An archaeometric approach to gain knowledge on technology and provenance of Apulian red figured pottery from Taranto. Archaeol Anthropol Sci. doi:10.1007/s12520-016-0345-9

Gulmini M, Appolonia L, Framarin P, Mirti P (2006) Compositional and technological features of glazed pottery from Aosta Valley (Italy): a SEM-EDS investigation. Anal Bioanal Chem 386:1815–1822

Gulmini M, Scognamiglio F, Roselli G, Vaggelli V (2015) Composition and microstructure of maiolica from the museum of ceramics in Ascoli Piceno: evidences by electron microscopy and microanalysis. Applied Physics A Material Science & Processing 120:1643–1652

Kretz R (1983) Symbols for rock-forming minerals. Am Mineral 68:277–279

Maggetti M (1982) Phase analysis and its significance for technology and origin. In: Archeological ceramics (eds.G. S. Olin and a. D. Franklin). Smithsonian Institution Press, Washington, DC, pp 121–133

Maggetti M, Neururer C, Ramseyer D (2011) Temperature evolution inside a pot during experimental surface (bonfire) firing. Appl Clay Sci 5:500–508

Mangone A, Giannossa LC, Ciancio A, Laviano R, Traini A (2008) Technological features of Apulian red figured pottery. J Archaeol Sci 35:1533–1541

Mangone A, Giannossa LC, Laviano R, Fioriello CS, Traini A (2009a) Late Roman lamps from Egnatia: from imports to local production. Investigations by various analytical techniques to the correct classification of archaeological finds and delineation of technological features. Microchem J 91:214–221

Mangone A, Giannossa LC, Laganara C, Laviano R, Traini A (2009b) Manufacturing expedients in medieval ceramics in Apulia. J Cult Herit 10:134–143

Mangone A, De Benedetto GE, Fico D, Giannossa LC, Laviano R, Sabbatini L, van der Werf I, Traini A (2011) Multianalytical study of archaeological faience from Vesuvian area as a valid tool to investigate provenance and technological features. New J Chem 35: 2860–2868

Mangone A, Caggiani MC, Giannossa LC, Eramo G, Redavid V, Laviano R (2013) Diversified production of red figured pottery in Apulia (southern Italy) in the late period. J Cult Herit 14:82–88

Maritan L, Nodari L, Mazzoli C, Milano A, Russo U (2006) Influence of firing conditions on ceramic products: experimental study on clay rich in organic matter. Appl Clay Sci 31:1–15

Mason RB, Tite MS (1997) The beginnings of tin-opacification of pottery glazes. Archaeometry 39:41–58

Mirti P, Gulmini M, Pace M, Elia D (2004) The provenance of red figure vases from Locri Epizephiri (southern Italy): new evidence by chemical analysis. Archaeom 46(2):183–200

Molera J, Pradell T, Salvado' N, Vendrell-Saz M (1999) Evidence of tin oxide recrystallization in opacified lead glazes. J Am Ceram Soc 82(10):2871–2875

Pouchou JL, Pichoir F (1988) Microbeam analysis. In: Newbury DE (ed) A simplified version of the ʙPAP^ model for matrix corrections in EPMA. San Francisco Press, San Francisco, pp 315–318

Pouchou JL, Pichoir F (1991) Quantitative analysis of homogeneous or stratified microvolumes applying the model ʙPAP^. In: Heinrich KFJ, Newbury DE (eds) Electron probe quantitation. Plenum Press, New York, pp 31–75

Riccardi MP, Messiga B, Duminuco P (1999) An approach to the dynamics of clay firing. Appl Clay Sci 15:393–409

Rotili M (1999) Archeologia del donjon di Montella. Arte Tipografica, Napoli

Rotili M (2011a) Protomajolica.In: Rotili M (ed) Montella: ricerche archeologiche nel ʙdonjon^ e nell'area murata (1980–92 e 2005–07), Arte Tipografica, Napoli, pp 300–311

Rotili M (2011b) Smaltata di transizione. In: Rotili M (ed) Montella: ricerche archeologiche nel/donjon/e nell'area murata (1980–92 e 2005–07). Arte Tipografica, Napoli, pp 311–315

Rotili M, Busino N (2017) Ricerche archeologiche nel castello di Ariano Irpino (1988–94, 2008). Edipuglia, Bari in press

Swann CP, Ferrence S, Betancourt PP (2000) Analysis of Minoan white pigments used on pottery from Palaikastro. Nucl Inst and Meth In Phys Res B 161-163:714–717

Vendrell M, Molera J, Tite MS (2000) Optical properties of tin-opacified glazes. Archaeometry 42:325–340